Inorg. Chem. **2002**, *41*, 2389–2399

Structural and Density Functional Studies of Uranium(III) and Lanthanum(III) Complexes with a Neutral Tripodal N-Donor Ligand Suggesting the Presence of a U–N Back-Bonding Interaction

Marinella Mazzanti,*,† Raphaël Wietzke,† Jacques Pécaut,‡ Jean-Marc Latour,§ Pascale Maldivi,*,† and Michael Remy†

Laboratoire de Reconnaissance Ionique, Service de Chimie Inorganique et Biologique (UMR 5046 CEA-CNRS-Université J. Fourier Grenoble), Département de Recherche Fondamentale sur la Matière Condensée, CEA-Grenoble, 38054 Grenoble Cedex 09, France, Laboratoire de Coordination et Chiralité, Service de Chimie Inorganique et Biologique (UMR 5046 CEA-CNRS-Université J. Fourier Grenoble), Département de Recherche Fondamentale sur la Matière Condensée, CEA-Grenoble, 38054 Grenoble Cedex 09, France, and Laboratoire de Physicochimie des Métaux en Biologie, Département de Biologie Moléculaire et Structurale, CEA-Grenoble, 38054 Grenoble Cedex 09, France

Received August 6, 2001

The crystal structures of two trisiodide octacoordinated uranium(III) complexes of tris[(2-pyrazinyl)methyl]amine (tpza), which differ only by the ligand occupying the eighth coordination site (thf or MeCN), and of their lanthanum(III) analogues have been determined. In the acetonitrile adducts the $M–N_{pyrazine}$ distances are very similar for U(III) and La(III), while the $U–N_{acetonitrile}$ distance is 0.05 Å shorter than the $La–N_{acetonitrile}$ distance. In the $[M(tpza)I_3(thf)]$ complexes in which the monodentate acetonitrile ligand, a weak π-acceptor ligand, is replaced by a thf molecule, a σ-donor only, the mean value of the distance $U–N_{pyrazine}$ is 0.05 Å shorter than the mean value of the $La–N_{pyrazine}$ distance. Since we are comparing isostructural compounds of ions with very similar ionic radii, these differences indicate the presence of a stronger M–N interaction in the U(III) complexes and therefore suggest the presence of a covalent contribution to the U–N bonding. The selectivity of the tpza ligand toward U(III) complexation (with respect to that of La(III)) in the presence of σ-donor-only ligands has been quantified by the value of $K_{U(tpza)}/K_{La(tpza)}$ measured to be 3.3 ± 0.5. The analysis of the metal–N-donor ligand bonding was carried out by a quasi-relativistic density functional theory study on small model compounds, of formula $I_3M–L$ (M = La, Nd, U; L = acetonitrile, pyrazine) and $I_3M–(pyrazine)_3$ (M = La, U). The structural data obtained from geometry optimizations on these systems reproduce experimental trends, i.e., a decrease in the M–N distance from La to U, combined with an increase of the C–N distance in the acetonitrile derivatives. A detailed orbital analysis carried out on the resulting optimized complexes did not reveal any orbital interaction between the trivalent lanthanide cations (Ln^{3+}) and the N-donor ligands. In contrast, a back-donation electron transfer from 5f U^{3+} orbitals to the π^* virtual orbital of the ligand was observed for both acetonitrile and pyrazine. Evaluation of the total bonding energy between the MI_3 and L fragments shows that this orbital interaction leads to a stabilization of the uranium(III) system compared to the lanthanide species.

Introduction

While bonding in f elements is traditionally described as essentially electrostatic, the issue of f covalency has often been a subject of debate in the past.[1–4] The presence of strong metal−ligand back-donation could explain the recently described formation of bisarene lanthanide(0) complexes and of uranium(III) carbonyl complexes which appear to violate

* To whom correspondence should be addressed. E-mail: mazzanti@drfmc.ceng.cea.fr.

† Laboratoire de Reconnaissance Ionique, Département de Recherche Fondamentale sur la Matière Condensée.

‡ Laboratoire de Coordination et Chiralité, Département de Recherche Fondamentale sur la Matière Condensée.

§ Laboratoire de Physicochimie des Métaux en Biologie, Département de Biologie Moléculaire et Structurale.

(1) Raymond, K. N.; Eigenbrot, C. W., Jr. *Acc. Chem. Res.* **1980**, *13*, 276.
(2) Burns, C. J.; Bursten, B. E. *Comments Inorg. Chem.* **1989**, *9*, 61.
(3) Sockwell, S. C.; Hanusa, T. P. *Inorg. Chem.* **1990**, *29*, 76.
(4) Freedman, D.; Melman, J. H.; Emge, T. J.; Brennan, J. G. *Inorg. Chem.* **1998**, *37*, 4162.

10.1021/ic010839v CCC: $22.00
Published on Web 04/05/2002

this predominantly electrostatic description of bonding.[5−7] The analysis of structural data for a large number of complexes[3,8] has been used to evaluate the degree of covalency of metal−ligand bonding in organoactinides. Structural evidence for U(III) to phosphorus π-back-bonding has been reported by Brennan and co-workers.[9] Spectroscopic evidence for covalency has also been described in a few cases.[10−12] A large number of computational studies of the electronic structure of organometallic complexes of low-valent actinides have been reported.[13,14] A wide variety of computational methods have been applied to investigate the nature of metal−ligand bonding in these compounds. In particular, Bursten and co-workers[15−17] have shown by Xα-SW calculations that $(Cp)_3U-L$ compounds (Cp = cyclopentadienyl), where L is a π-acidic ligand such as CO or NO, present back-donation from U($5f^3$) valence orbitals to the virtual π^* orbital of the π-acceptor ligand.

Much fewer computational or structural studies have been done on nonorganometallic complexes of trivalent actinides. Indeed the coordination chemistry of trivalent actinides is poorly developed.[18−23] A few complexes of U(III) with tripodal anionic N-donor ligands have been crystallographically characterized in the past.[24−26] Among these, a complex containing a tripodal amido ligand reacts with molecular nitrogen to form a dinitrogen complex.[26] While the structural data do not show a lengthening of the N_2 bond, investigation of the electronic structure of the dinitrogen complex $[\{(NH_2)_3(NH_3)U\}_2(\mu^2\text{-}\eta^2\text{:}\eta^2\text{-}N_2]$ by density functional theory (DFT) calculations has shown evidence for a back-donation

Chart 1

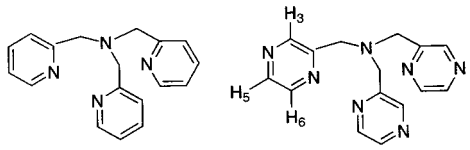

tpa tpza

interaction from U($5f^3$) to the N_2 π^* virtual orbital.[27] Ligands containing aromatic nitrogens as donor atoms have been reported to complex actinides(III) more strongly than lanthanides(III), owing to a greater covalent contribution to the metal−nitrogen bonding.[28,29] In particular we have shown that tripodal oligoamines such as tris[(2-pyridyl)methyl]-amine (tpa) and tris[(2-pyrazinyl)methyl]amine (tpza) (Chart 1) extract actinides selectively in preference to lanthanides from nitric acid solutions into an organic phase, with the ligand tpza displaying a higher selectivity than tpa. This behavior could be explained by the softer character of tpza, which is expected to give rise to a stronger interaction with the actinides. However, there is no experimental or computational evidence of the covalent character of the An(III)−aromatic nitrogen bonding, despite the potential application of heterocyclic imines in actinide(III)/lanthanide(III) separation,[30−34] a difficult problem in nuclear waste disposal.[35−39] To assess possible differences in An(III) vs Ln(III) bonding to aromatic nitrogen donors, we are investigating the complexation of actinides(III) and lanthanides(III) with tripodal aromatic amines.

To relate possible structural differences between La(III) and U(III) complexes with the presence of a larger degree of covalency in the U(III)−ligand interaction, we compare isostructural complexes of La and U containing the same

(5) Brennan, J. G.; Andersen, R. A.; Robbins, J. L. *J. Am. Chem. Soc.* **1986**, *108*, 335.
(6) Cloke, F. G. N. *Chem. Soc. Rev.* **1993**, 17.
(7) Parry, J.; Carmona, E.; Simon, C.; Hursthouse, M. *J. Am. Chem. Soc.* **1995**, *117*, 2649.
(8) Brennan, J. G.; Stults, S. D.; Andersen, R. A.; Zalkin, A. *Inorg. Chim. Acta* **1987**, *139*, 201.
(9) Brennan, J. G.; Stults, S. D.; Andersen, R. A.; Zalkin, A. *Organometallics* **1988**, *7*, 1329.
(10) Conejo, M. d. M.; Parry, J. S.; Carmona, E.; Schultz, M.; Brennan, J.; Beshouri, S. M.; Andersen, R. A.; Rogers, R. D.; Coles, S.; Hursthouse, M. *Chemistry* **1999**, *5*, 3000.
(11) Kaltsoyannis, N.; Bursten, B. E. *J. Organomet. Chem.* **1997**, *528*, 19.
(12) Brennan, J., G.; Green, J. C.; Redfern, C. M. *J. Am. Chem. Soc.* **1989**, *111*, 2373.
(13) Pepper, M.; Bursten, B. E. *Chem. Rev.* **1991**, *91*, 719.
(14) Kaltsoyannis, N. *J. Chem. Soc., Dalton Trans.* **1997**, 1.
(15) Bursten, B. E.; Strittmatter, R. J. *Angew. Chem., Int. Ed. Engl.* **1991**, *30*, 1069.
(16) Bursten, B. E.; Strittmatter, R. J. *J. Am. Chem. Soc.* **1987**, *109*, 6606.
(17) Bursten, B. E.; Rhodes, L. F.; Strittmatter, R. J. *J. Am. Chem. Soc.* **1989**, *111*, 2758.
(18) Cotton, S. *Lanthanides and Actinides*; MacMillan Education: London, 1991.
(19) Santos, I.; Pires de Matos, A.; Maddock, A. G. *Adv. Inorg. Chem.* **1989**, *34*, 65.
(20) Stewart, J. L.; Andersen, R. A. *New J. Chem.* **1995**, *19*, 587.
(21) Avens, L. R.; Bott, S. G.; Clark, D. L.; Sattelberger, A. P.; Watkin, J. G.; Zwick, B. D. *Inorg. Chem.* **1994**, *33*, 2248.
(22) Van Der Sluys, W. G.; Burns, C. J. *J. Am. Chem. Soc.* **1988**, *110*, 5924.
(23) Maria, L.; Campello, M. P.; Domingos, A.; Santos, I.; Andersen, R. *J. Chem. Soc., Dalton Trans.* **1999**, 2015.
(24) Amoroso, A. J.; Jeffery, J. C.; Jones, P. L.; McCleverty, J. C.; Rees, L.; Rheingold, A. L.; Sun, Y.; Takats, J.; Trofimenko, S.; Ward, M. D.; Yap, G. P. A. *J. Chem. Soc., Chem. Commun.* **1995**, 1881.
(25) Carvalho, A.; Domingos, A.; Gaspar, P.; Marques, N.; Pires de Matos, A.; Santos, I. *Polyhedron* **1992**, *11*, 1481.
(26) Roussel, P.; Scott, P. *J. Am. Chem. Soc.* **1998**, *120*, 1070.
(27) Kaltsoyannis, N.; Scott, P. *Chem. Commun.* **1998**, 1665.
(28) Wietzke, R.; Mazzanti, M.; Latour, J.-M.; Pecaut, J.; Cordier, P.-Y.; Madic, C. *Inorg. Chem.* **1998**, *37*, 6690.
(29) Musikas, C. In *Actinide/lanthanide group separation using sulfur and nitrogen donor extractants*; Musikas, C., Ed.; World Scientific: Singapore, 1984; p 19.
(30) Cordier, P.-Y.; Hill, C.; Baron, P.; Madic, C.; Hudson, M.; Liljenzin, J. O. *J. Alloys Compds.* **1998**, *271−273*, 738.
(31) Kolarik, Z.; Müllich, U.; Gassner, F. *Solvent Extr. Ion Exch.* **1999**, *17*, 23.
(32) Kolarik, Z.; Müllich, U.; Gassner, F. *Solvent Extr. Ion Exch.* **1999**, *17*, 1155.
(33) Drew, M. G. B.; Iveson, P. B.; Hudson, M. J.; Liljenzin, J. O.; Spjuth, L.; Cordier, P.-Y.; Enarsson, A.; Hill, C.; Madic, C. *J. Chem. Soc., Dalton Trans.* **2000**, 821.
(34) Drew, M. G. B.; Hudson, M. J.; Iveson, P. B.; Madic, C.; Russel, M. *J. Chem. Soc., Dalton Trans.* **2000**, 2711.
(35) Nash, K. L. In *Handbook on the Physics and Chemistry of Rare Earth*; Gschneidner, K. A., Jr., Eyring, L., Choppin, G. R., Lander, G. H., Eds.; Elsevier Science B.V.: Amsterdam, 1994; Vol. 18.
(36) *Actinides and Fission Products Partitioning and Transmutation, Status and Assessment Report*, Proceedings of the Fifth International Information Exchange Meeting, Mol, Belgium, Nov 25−27, 1998; NEA/OECD Report; NEA/OECD: Paris, 1999.
(37) Kolarik, Z. *Separation of Actinides and Long-Lived Fission Products from High-level Radioactive Wastes (a review)*; Kernforschungszentrum: Karlsruhe, Germany, 1991.
(38) Jarvinen, G. D. *Chemical Separation Technologies and Related Methods of Nuclear Waste Management*; Kluwer Academic Publishers: Dordrecht, The Netherlands, 1999.
(39) Arthur, E. D.; Rodriguez, A.; Schriber, S. O. In *AIP Conference Proceedings 346*; Arthur, E. D., Rodriguez, A., Schriber, S. O., Eds.; AIP Press: Woodbury, NY, 1995.

iodide counterion. In a previous study small differences in the metal−nitrogen distances were found in the isostructural complexes of tpa [M(tpa)I_3(py)] (M = La, U).[40] Here we report the synthesis, the solution-state structure, and the crystallographic characterization of the iodide complexes of La(III) and U(III) with the softer ligand tpza, which is expected to give more covalent bonding than tpa.

Moreover, to gain detailed information about the bonding between the La(III) or U(III) cations and N-donor ligands such as acetonitrile or pyrazine, we have also performed electronic structure calculations on model systems using the Kohn−Sham formalism of DFT. The potential of modern DFT methods, including gradient generalized approximation (GGA) or hybrid DFT/Hartree−Fock (HF) functionals, has recently been established, both for complexes of d metals[41,42] and for complexes of f elements.[43−46] Moreover, the analysis of the electron density gives a straightforward "chemical" description of the bonding, due to the monodeterminantal nature of this methodology. The significant differences that we observe between La−N and U−N distances are discussed in light of such computational studies, carried out on the model systems [MI_3] for M = La, Nd, and U and L = pyrazine and acetonitrile and [M(pyrazine)$_3I_3$] for M = La and U.

Experimental Section

General Details. ^{1}H NMR spectra were recorded on Bruker AM-400, Bruker AC-200, and Varian U-400 spectrometers using deuterated C_5D_5N, d_8-THF, and CD_3CN solvents with C_5H_5N, THF, and CH_3CN as internal standards. All manipulations were carried out under an inert argon atmosphere using Schlenk techniques and a Braun glovebox equipped with a purifier unit. The water and oxygen levels were always maintained at less than 1 ppm. All solvents including deuterated solvents were purchased from Aldrich in their anhydrous form, conditioned under argon, and vacuum distilled from K (pyridine, tetrahydrofuran, hexane) or CaH_2 (acetonitrile). Depleted uranium turnings were purchased from the "Societé Industrielle du Combustible Nucleaire". Solid or solution samples of the uranium complexes were stored in the glovebox in glass vessels sealed with silicon-greased stoppers. Elemental analyses were performed under argon by SCA/CNRS, Vernaison, France. Starting materials were purchased from Aldrich, Fluka, and Alfa and used without further purification unless otherwise stated. LaI_3 anhydrous beads were purchased from Aldrich. The ligand tpza was prepared as previously described.[28] $UI_3(thf)_4$ was prepared as described by Clark and co-workers.[21] [LaI_3(thf)$_4$] was prepared by stirring anhydrous beads of LaI_3 in thf overnight. The white powder obtained after filtration was purified by extraction in hot thf.

X-ray-quality white crystals of [La(tpza)I_3(MeCN)]·MeCN, **1**, and dark green crystals of [U(tpza)I_3(MeCN)]·MeCN, **2**, were obtained by slow diffusion of *n*-hexane into a solution of $MI_3(thf)_4$ and tpza (in a 1:1 ratio) in a 1:3 thf/acetonitrile mixture. The value of the $K_{U(tpza)}/K_{La(tpza)}$ ratio was obtained from seven independent experiments.

Table 1. ^{1}H NMR Chemical Shifts for tpza Complexes in Various Deuterated Solvents

solvent	compound	H^6	H^5	H^3	CH_2
pyridine	tpza				
	La(tpza)I_3	9.54	8.52	8.34	4.82
	U(tpza)I_3	23.84	10.16	10.83	−2.38
thf	tpza	8.53	8.48	8.87	4.02
	La(tpza)I_3	9.56	8.61	8.64	4.65
	U(tpza)I_3	26.12	10.01	10.01	−2.60
CD_3CN	tpza	8.53	8.47	8.78	4.00
	La(tpza)I_3	9.31	8.64	8.70	4.55
	U(tpza)I_3	19.79	9.08	9.55	−1.27

Synthesis of [M(tpza)I_3(thf)]·thf (M = La, 3; M = U, 4). A solution of tpza (20 mg, 0.068 mmol) in thf (2 mL) was added to a solution of $MI_3(thf)_4$ (0.068 mmol) in thf (2 mL). After the solution was left at −20 °C overnight, white (La) or dark blue (U) microcrystalline solids were obtained (60−70% yeld). Anal. Calcd for [U(tpza)I_3(thf)], $UC_{19}H_{23}ON_7I_3$: C, 23.16; H, 2.33; N, 9.95. Found: C, 23.18; H, 2.51; N, 9.76. Anal. Calcd for [La(tpza)I_3-(thf)], $LaC_{19}H_{23}ON_7I_3$: C, 25.75; H, 2.59; N, 11.07. Found: C, 25.85; H, 2.64; N, 10.89.

^{1}H NMR chemical shifts of the tpza complexes are given in Table 1.

Computational Details. All computations have been carried out in the Kohn−Sham (KS) formalism of DFT. Relativistic effects were taken into account through the scalar quasi-relativistic methodology developed in the Amsterdam density functional package (ADF 1999).[47] Frozen core densities were computed by relativistic Dirac−Slater calculations for all atoms, and then the valence electron density was computed by a quasi-first-order perturbative treatment of the main relativistic terms (i.e., mass−velocity and Darwin) developed upon nonrelativistic Slater-type orbitals (STOs). The valence space was the following: La [] $5s^2$ $5p^6$ $6s^2$ $5d^1$, U [] $6s^2$ $6p^6$ $7s^2$ $5f^3$ $6d^1$, I [] $5s^2$ $5p^5$, C [] $2s^2$ $2p^2$, and O [] $2s^2$ $2p^3$. The basis sets used Slater triple-ζ functions for the f elements, and triple-ζ functions plus one polarization d function for the other atoms. Auxiliary sets of STOs were used to fit the electron density, and to generate the Coulomb potential.[48]

The exchange and correlation potentials were included self-consistently, through the GGA scheme, with a local part using the parametrization of Vosko, Wilk, and Nusair for the correlation[49] and the uniform electron gas for exchange, and with the gradient correction of Becke[50] for exchange and of Perdew[51] for correlation.

The spin polarization for Nd(III) and U(III) complexes was determined on the basis of the weak field approach, which is valid for f elements. The application of Hund's rules on the f^3 electron configuration of the free Nd^{3+} and U^{3+} cations thus leads to a quartet ground state. A spin polarization of 3 was therefore used for Nd(III) and U(III) species, within an unrestricted formalism.

The generalized transition-state procedure of Ziegler et al.,[52] as implemented in ADF, was used, taking advantage of the fragment-based construction of the molecule. The various energetic terms contributing to the total bonding energy (E_{TBE}) are, first, the steric

(40) Wietzke, R.; Mazzanti, M.; Latour, J.-M.; Pecaut, J. *J. Chem. Soc., Dalton Trans.* **2000**, 4167.
(41) Chermette, H. *Coord. Chem. Rev.* **1998**, *178/179/180*, 699.
(42) Bauschlicher, C. W.; Ricca, A.; Partridge, H.; Langhoff, S. *Recent Advances in Density Functional Theory*; World Scientific Publishing: Singapore, 1997.
(43) Adamo, C.; Maldivi, P. *J. Phys. Chem. A* **1998**, *102*, 6812.
(44) Ziegler, T.; Tschinke, V.; Baerends, E. J.; Snijders, J. G.; Ravenek, W. *J. Phys. Chem.* **1989**, *93*, 3050.
(45) Hay, P. J.; Martin, R. L. *J. Chem. Phys.* **1998**, *109*, 3875.
(46) Joubert, L.; Maldivi, P. *J. Chem. Phys. A* **2001**, *105*, 9068.
(47) Yang, L.-W.; Liu, S.; Rettig, S. J.; Orvig, C. *Inorg. Chem.* **1995**, *34*, 4921.
(48) te Velde, G.; Baerends, E. J. *J. Comput. Chem.* **1992**, *99*, 84.
(49) Vosko, S. H.; Wilk, L.; Nusair, M. *Can. J. Phys.* **1980**, *58*, 1200.
(50) Becke, A. D. *Phys. Rev. A* **1988**, *38*, 3098.
(51) Perdew, J. P. *Phys. Rev. B* **1986**, *33*, 8822.
(52) Ziegler, T.; Rauk, A. *Theor. Chim. Acta* **1977**, *46*, 1.

Table 2. Crystallographic Data for the Four Structures

	1	2	3	4
empirical formula	$C_{19}H_{21}N_9I_3La$	$C_{19}H_{21}N_9I_3U$	$C_{23}H_{31}I_3N_7O_2La$	$C_{23}H_{31}I_3N_7O_2U$
fw	895.06	994.18	957.16	1056.28
cryst syst	triclinic	triclinic	monoclinic	monoclinic
space group	$P\bar{1}$	$P\bar{1}$	$P2(1)/c$	$P2(1)/c$
a, Å	9.8436(6)	9.950(2)	13.7258(7)	13.6903(12)
b, Å	12.2206(8)	12.190(2)	10.1425(5)	10.0753(9)
c, Å	14.3700(10)	14.440(3)	22.7976(12)	22.586(2)
α, Å	111.7590(10)	111.41(3)	90	90
β, Å	92.4440(10)	92.07(3)	105.9150(10)	105.855(2)
γ, Å	108.9560(10)	109.17(3)	90	90
V, Å^3/Z	1492.01(17)/2	1515.7(5)/2	3052.1(3)/4	2996.9(5)/4
D_{calcd}, g cm^{-3}	1.992	2.178	2.083	2.341
μ(Mo Kα), mm^{-1}	4.557	8.431	4.466	8.539
temp, K	193(2)	143(2)	193(2)	143(2)
no. of params refined	289	289	463	325
no. of reflns collected/obsd ($I > 2\sigma(I)$)	9731/5957	9538/5294	19059/6677	19101/6065
R1, wR2[a]	0.0518, 0.1400	0.0572, 0.1469	0.0239, 0.0597	0.0602, 0.1526

[a] The structure was refined on F_o^2 using all data: wR2 = $[\sum[w(F_o^2 - F_c^2)^2]/\sum w(F_o^2)^2]^{1/2}$, where $w^{-1} = [\sigma(F_o^2) + (aP)^2 + bP]$ and $P) + 2F_c^2]/3$.

term (E_{ster}), which is the sum of the electrostatic interaction and of the Pauli repulsion between the electron densities of the starting fragments when they are put together in the molecular geometry. The second term, describing the orbital interaction, arises from the energy gain when electronic convergence is achieved to self-consistency, and thus contains both intramolecular (i.e., polarization) and intermolecular (i.e., electron transfer) fragment orbital interactions. To summarize, the total bonding energy may be written as $E_{TBE} = E_{ster} + E_{orb}$, with $E_{ster} = E_{elect} + E_{Pauli.}$

Orbital representations have been drawn using the Molden program,[53] and we used the ADFrom code, developed by F. Mariotti and A. Bencini at the University of Florence (see the Web site http://www-chem.unifr.ch/ac/phd/fmariotti/ADFrom.html) to read the binary output files of ADF.

X-ray Crystallography. All diffraction data were taken using a Bruker SMART CCD area detector three-circle diffractometer (Mo Kα radiation, graphite monochromator, $\lambda = 0.71073$ Å). To prevent oxidation and solvent loss, the crystals were mounted in a capillary tube in the glovebox and quickly transferred to a stream of cold nitrogen on the diffractometer.

The cell parameters were obtained with intensities detected on 3 batches of 15 frames with a 10 s exposure time for each. The crystal−detector distance was 5 cm. For three settings of ϕ and 2θ, 1200 narrow data frames were collected for 0.3° increments in ω. A full hemisphere of data was collected for each complex. At the end of data collection, the first 50 frames were recollected to establish that crystal decay had not taken place during the collection. Unique intensities with $I > 10\sigma(I)$ detected on all frames using the Bruker SMART program[54] were used to refine the values of the cell parameters. The substantial redundancy in data allows empirical absorption corrections to be applied using multiple measurements of equivalent reflections with the SADABS Bruker program;[54] space groups were determined from systematic absences, and they were confirmed by the successful solution of the structure (see Table 2). Complete information on crystal data and data collection parameters is given in the Supporting Information.

The structures were solved by direct methods using the SHELXTL 5.03 package,[55] and all atoms were found by difference Fourier syntheses. All non-hydrogen atoms were anisotropically refined on F^2. Hydrogen atoms were included in calculated positions and refined isotropically.

Results

Solution Structure of tpza Complexes. The proton NMR spectra of 1:1 acetonitrile or tetrahydrofuran solutions of $MI_3(thf)_4$ (M = La, U) and tpza show the presence (Table 1) of one set of signals with three signals for the nine pyrazine protons and one signal for the six methylene protons, indicating a 3-fold symmetry in which all chelating arms of the tpza ligand are equivalent. It follows that the solvent molecule (thf or acetonitrile) coordinated to the metal is exchanging rapidly with the bulk solvent. The presence of only one signal for the methylene is in agreement with the presence in solution of a C_{3v} symmetric species. The attribution of the signals was confirmed by two-dimensional COSY spectroscopy.

At L:M ratios larger than 2 the NMR spectra in acetonitrile or thf show the peaks of the 1:1 complex and of the free ligand. This shows that, while for tpa the formation of bisligand complexes $[M(tpa)_2]I_3$ (M = La(III), U(III)) has been observed in acetonitrile and in pyridine,[40] tpza only forms 1:1 complexes. The NMR spectra of 1:1 pyridine solutions ($\sim 10^{-2}$ M) of $MI_3(thf)_4$ (M = La, U) and tpza show the presence of two sets of signals which were attributed to the 1:1 complex and to the free ligand. In a previous study we had observed that the complexes $[M(tpa)(py)I_3]$ (M = La(III) and U(III)) do not undergo dissociation of the tripodal ligand tpa in pyridine solution ($\sim 10^{-2}$ M).[40] The lower stability of the $[M(tpza)I_3]$ complexes toward ligand dissociation in pyridine with respect to the analogous tpa complexes and the lack of formation of bisligand complexes for tpza indicate that tpza binds La^{3+} and U^{3+} less strongly than tpa in agreement with its lower σ-donor ability.[28] The values of the formation constants for the tpza complexes of La and U in pyridine, obtained from the integration of NMR signals, are very similar within experimental uncertainties ($K_f = 175 \pm 20$ mol^{-1} L for U and 188 ± 20 mol^{-1} L for La). The NMR spectra of 1:1:1 thf solutions of $LaI_3(thf)_4$/$UI_3(thf)_4$/tpza show the presence of two sets of signals which

(53) Schaftenaar, G.; Noordik, J. H. *J. Comput.-Aided Mol. Des.* **2000**, *14*, 123.
(54) SMART *Software package for use with the SMART diffractometer*; Bruker: Madison, WI, 1995.
(55) Sheldrick, G. M. In *SHELXTL-Plus*, 5th ed.; Sheldrick, G. M., Ed.; University of Göttingen: Göttingen, Germany, 1994.

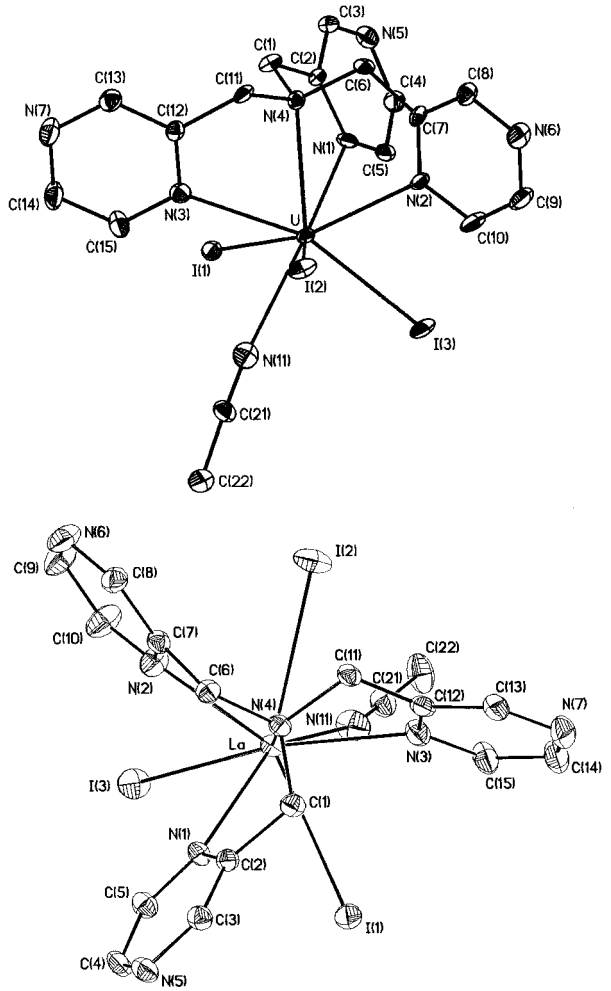

Figure 1. (a, top) Side view of the crystal structure of the complex [U(tpza)I_3(MeCN)], **2**, and (b, bottom) top view of the crystal structure of the complex [La(tpza)I_3(MeCN)], **1**, with thermal ellipsoids at 30% probability.

were assigned to the U(III) and La(III) complexes of tpza. The integration of the signals corresponding to the U(tpza) and La(tpza) complexes allows the determination of the ratio of the formation constants of the two 1:1 complexes. The value of the ratio $K_{U(tpza)}/K_{La(tpza)}$ measured to be 3.3 ± 0.5 shows that, while in pyridine tpza does not display any selectivity toward the complexation of U(III), in thf tpza binds the U(III) ion more strongly than the La(III) ion.

Crystal and Molecular Structure of tpza Complexes. The crystal structures of the isostructural complexes **1** and **2** are shown in Figure 1. Selected interatomic distances and angles are given in Table 3. The metal is eight-coordinated by four nitrogens of the tpza ligand, three iodides, and one acetonitrile molecule. The metal environment can be described as a distorted square antiprism, with N1, N4, N3, and I1 forming one square plane (mean deviation 0.08 Å for U and 0.06 Å for La) and N2, N11, I2, and I3 occupying the second plane (0.40 Å for U and 0.41 Å for La). The angle between the two square planes is 7.1° for the U(III) complex and 6.9° for the La(III) complex. The La−N distances range from 2.662(6) to 2.723(5) Å, and the U−N distances range from 2.610(10) to 2.726(8) Å, with the shorter distance belonging to the acetonitrile molecule. These

Table 3. Selected Bond Distances (Å) and Angles (deg) in **1** and **2**

	2	**1**	ΔLa−U
M−N(1)	2.726(8)	2.723(5)	−0.003
M−N(2)	2.685(8)	2.692(6)	0.007
M−N(3)	2.672(8)	2.691(5)	0.019
M−N(4)	2.721(8)	2.715(4)	−0.006
M−N(11)	2.610(10)	2.662(6)	0.052
M−I(3)	3.1632(10)	3.1465(5)	−0.017
M−I(1)	3.2383(14)	3.2342(5)	−0.0041
M−I(2)	3.2637(10)	3.2472(5)	−0.0165
N(11)−C(21)	1.193(14)	1.130(9)	−0.063
N(11)−M−N(3)	81.0(3)	81.57(19)	
N(11)−M−N(2)	131.2(3)	131.50(19)	
N(3)−M−N(2)	118.9(3)	117.90(16)	
N(11)−M−N(4)	143.2(3)	142.96(18)	
N(3)−M−N(4)	64.1(2)	63.49(15)	
N(2)−M−N(4)	64.4(2)	63.72(15)	
N(11)−M−N(1)	144.1(3)	144.65(17)	
N(3)−M−N(1)	104.9(2)	103.63(15)	
N(2)−M−N(1)	77.5(3)	77.46(17)	
N(4)−M−N(1)	62.3(2)	61.76(14)	
N(11)−M−I(3)	81.6(2)	82.15(15)	
N(3)−M−I(3)	160.23(18)	161.24(12)	
N(2)−M−I(3)	79.96(18)	80.13(11)	
N(4)−M−I(3)	134.60(17)	134.21(10)	
N(1)−M−I(3)	84.00(17)	84.59(10)	
N(11)−M−I(1)	76.8(2)	76.22(14)	
N(3)−M−I(1)	77.09(19)	77.18(11)	
N(2)−M−I(1)	147.18(19)	147.82(13)	
N(4)−M−I(1)	104.81(17)	105.62(10)	
N(1)−M−I(1)	70.39(18)	71.14(10)	
I(3)−M−I(1)	89.82(4)	89.944(14)	
N(11)−M−I(2)	72.7(2)	72.66(14)	
N(3)−M−I(2)	75.27(18)	75.82(11)	
N(2)−M−I(2)	71.01(19)	70.67(13)	
N(4)−M−I(2)	86.63(17)	86.51(10)	
N(1)−M−I(2)	143.15(17)	142.68(10)	
I(3)−M−I(2)	108.28(3)	107.952(15)	
I(1)−M−I(2)	141.44(3)	141.170(17)	
C(21)−N(11)−M	169.9(9)	166.9(6)	
N(11)−C(21)−C(22)	176.5(13)	179,1(8)	

values are in the range of the La−N (2.79−2.60 Å)[56−58] and U−N (2.98−2.63)[24,56] distances reported in the literature. The tetradentate tpza adopts a helicoidal pseudo-C_3-symmetric arrangement. In both complexes one $M-N_{pyrazine}$ (M−N1) distance is longer than the other two and is also longer than the $M-N_{apical\ tertiary\ amine}$ (M−N4) distance. The average $M-N_{tpza}$ distance is the same for the two metals, while the M−N≡CCH_3 distance is significantly shorter in the uranium complex (2.610(10) Å for U and 2.662(4) Å for La). Similar metal−nitrogen distances have been reported for the uranium(III) nitrile complex [U(Cp)$_3$(NC^{n}Pr)] (2.61(1) Å)[59] and for the La(III) complex [La(Cp)$_3$(NCEt)] (2.657(5) Å).[60] The values of the M−N≡C and N≡C−C angles are in the range of those found for organonitriles coordinated in end-on fashion.[61]

A significant lengthening of the N≡C bond of the acetonitrile molecule is observed in the U complex

(56) Wietzke, R.; Mazzanti, M.; Latour, J.-M.; Pecaut, J. *J. Chem. Soc., Dalton Trans.* **1998**, 4087.
(57) Fréchette, M.; Bensimon, C. *Inorg. Chem.* **1995**, *34*, 3520.
(58) Fréchette, M.; Butler, I. R.; Hynes, R.; Detellier, C. *Inorg. Chem.* **1992**, *31*, 1650.
(59) Adam, R.; Villiers, C.; Ephritikine, M.; Lance, M.; Nierlich, M.; Vigner, J. *J. Organomet. Chem.* **1993**, *445*, 99.
(60) Spirlet, M. R.; Rebizant, J.; Apostolidis, C.; Kanellakopulos, B. *Inorg. Chim. Acta* **1987**, *139*, 211.
(61) Endres, H. *Comphrehensive Coordination Chemistry*; Pergamon Press: Oxford, 1987; Vol. 2, Ligands.

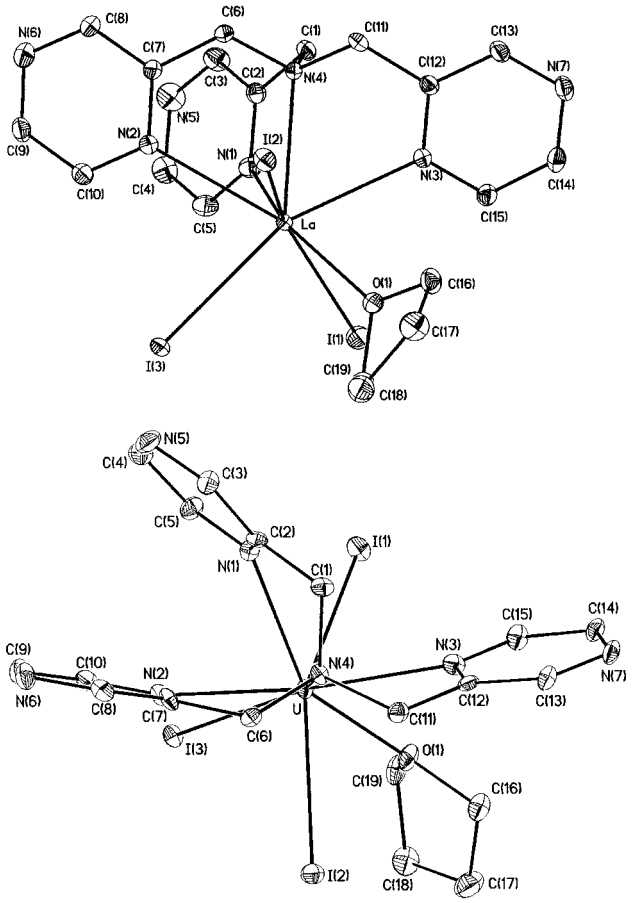

Figure 2. (a, top) Side view of the crystal structure of the complex [La(tpza)I_3(thf)], **3**, and (b, bottom) top view of the crystal structure of the complex [U(tpza)I_3(thf)], **4**, with thermal ellipsoids at 30% probability.

(1.193(14) Å) with respect to the La complex (1.130(9) Å). The N≡C bond length usually shortens on coordination, with values ranging from 1.11 to 1.15 Å in coordinated nitriles compared to 1.16 Å in free MeCN.[61] A value of 1.137(6) Å was found for the N≡C bond length in the complex [U(Cp)$_3$(NC^{n}Pr)].

X-ray-quality white crystals of [La(tpza)I_3(thf)]·thf, **3**, and dark blue crystals of [U(tpza)I_3(thf)]·thf, **4**, were obtained by slow diffusion of a 10^{-3} M tetrahydrofuran solution of tpza in a 10^{-3} M tetrahydrofuran solution of $MI_3(thf)_4$ (M = U, La). The crystal structures of the isostructural complexes **3** and **4** are shown in Figure 2. Selected interatomic distances and angles are given in Table 4. The coordination geometry around the U(III) and La(III) ions can be seen as a dodecahedron formed by the tetradentate ligand tpza, three iodides, and a thf molecule. The pseudo-C_3 symmetry of tpza is disrupted in these complexes by the inversion of the orientation of the pyrazinyl arm containing N2 (relative to that of the complexes **1** and **2**). This inversion arises from the presence of the thf (bulkier than MeCN), which results in a closer proximity of I(2) to the plane defined by the atoms N(1), N(2), and N(3) in the thf adducts (0.58 Å for U and 0.63 Å for La) with respect to the acetonitrile adducts (0.88 Å for U and 0.92 Å for La). In both types of adducts the distances of I(3) and I(4) from the N(1)N(2)N(3) plane are much longer (2.10−3.68 Å). A similar inversion of one arm

Table 4. Selected Bond Distances (Å) and Angles (deg) in **3** and **4**

	4	**3**	ΔLa−U
M−N(1)	2.669(8)	2.716(2)	0.047
M−N(2)	2.756(7)	2.798(2)	0.042
M−N(3)	2.657(7)	2.705(2)	0.048
M−N(4)	2.685(6)	2.732(2)	0.047
M−O(1)	2.542(7)	2.5668(19)	0.025
M−I(3)	3.1439(6)	3.1771(3)	0.0332
M−I(1)	3.1914(6)	3.2241(3)	0.0337
M−I(2)	3.2087(7)	3.2411(3)	0.0324
O(1)−M−N(3)	71.8(2)	73.03(7)	
O(1)−M−N(1)	147.2(2)	147.47(7)	
N(3)−M−N(1)	91.7(2)	90.47(7)	
O(1)−M−N(4)	125.3(2)	125.59(6)	
N(3)−M−N(4)	62.0(2)	61.30(6)	
N(1)−M−N(4)	64.0(2)	63.45(7)	
O(1)−M−N(2)	149.8(2)	150.17(7)	
N(3)−M−N(2)	125.9(2)	124.33(6)	
N(1)−M−N(2)	62.4(2)	61.90(7)	
N(4)−M−N(2)	63.99(19)	63.12(6)	
O(1)−M−I(3)	86.08(13)	86.64(5)	
N(3)−M−I(3)	157.10(16)	158.76(5)	
N(1)−M−I(3)	104.52(16)	104.16(5)	
N(4)−M−I(3)	139.90(14)	139.20(4)	
N(2)−M−I(3)	76.55(14)	76.65(5)	
O(1)−M−I(1)	75.86(15)	75.83(5)	
N(3)−M−I(1)	82.93(15)	82.74(5)	
N(1)−M−I(1)	74.07(16)	74.38(5)	
N(4)−M−I(1)	122.58(13)	122.38(4)	
N(2)−M−I(1)	126.30(16)	126.55(5)	
I(3)−M−I(1)	86.029(15)	86.436(6)	
O(1)−M−I(2)	74.83(15)	74.93(5)	
N(3)−M−I(2)	89.51(15)	89.60(5)	
N(1)−M−I(2)	134.71(16)	134.12(5)	
N(4)−M−I(2)	77.04(14)	76.73(5)	
N(2)−M−I(2)	80.71(16)	80.75(5)	
I(3)−M−I(2)	90.362(15)	91.005(6)	
I(1)−M−I(2)	150.64(2)	150.754(7)	

of the tripodal ligand has already been observed for the complex [Nd(tpa)Cl_3(MeOH)] with respect to the complexes [Ln(tpa)Cl_3] (Ln = Eu, Tb, Lu).[28] In the Nd complex the distance of the chloride ligand Cl(3) from the plane defined by the atoms N(1), N(2), and N(3) is 0.62 Å.

The M−N distances range from 2.705(2) to 2.798(2) Å for La and from 2.657(7) to 2.756(7) Å for U, with the longest distance belonging to one of the pyrazine nitrogens. While in the acetonitrile adducts of the tpza complexes (**1** and **2**) the average M−N_{tpza} distances are essentially the same for U and La, in the thf adducts the average M−N_{tpza} distances are significantly shorter (0.046 Å) for the U(tpza) complex than for the La(tpza) complex. This result suggests the presence of a stronger metal−tpza interaction for the U ion with respect to the La ion in the tpza complexes containing the ligand thf, which can only act as a σ-donor. The fact that in the acetonitrile adducts the M−tpza distances are the same for U and La while the M−$N_{acetonitrile}$ distances are shorter for U than for La indicates that the acetonitrile ligand, which can act as a π-acceptor, competes with tpza for the electron back-donation from the U ion.

Density Functional Calculations of Model Complexes [M(pyrazine)I_3] and [M(MeCN)I_3] for M = La, Nd, and U. The stability and molecular structures of the complexes **1**−**4** result from the mutual influence of several metal−ligand interactions. To develop a theoretical description of an "intrinsic" metal−ligand bond, independently of the rest of

Table 5. Calculated Metal−Ligand Bond Lengths (Å) and C−N Distances (Å) for MI_3–L (M = La, Nd, U; L = acetonitrile, pyrazine) Complexes[a]

L	complex	M−N	C−N
acetonitrile			1.16
	LaI_3–L	2.59 (2.66)	1.16 (1.13)
	NdI_3–L	2.52	1.16
	UI_3–L	2.26 (2.61)	1.18 (1.19)
pyrazine	LaI_3–L	2.63 (2.74)	1.35 (1.34)
	NdI_3–L	2.55	1.35
	UI_3–L	2.32 (2.59)	1.37 (1.34)

[a] Experimental values are given in parentheses.

the coordination sphere, we have chosen to study simple model systems. They consist of a trivalent metal cation, M^{3+}, interacting with the N-donor ligand (acetonitrile or pyrazine), plus three iodide counterions, as in the experimental structures. In the case of the acetonitrile ligand, we have only explored the η^1 coordination mode through the N atom of the nitrile to reproduce the bonding geometry observed in the experimental structures. We have chosen to investigate these model systems with M = La(III) and U(III) because of their very similar ionic radii (which differ by 0.007 Å[62]) and because of the availability of the experimental structural data, and also with Nd(III) ($4f^3$), the lanthanide isoelectronic to U(III) ($5f^3$).

Geometry optimizations of these model compounds have been carried out in internal coordinates with all parameters free except for the flatness of the pyrazine ring. A bonding analysis was then carried out, both by the examination of the resulting Kohn−Sham orbitals and by an energetic decomposition of electrostatic and polarization/charge-transfer terms, as implemented in ADF through the generalized transition-state method of Ziegler et al.[52]

The metal−ligand distances and the C−N distance of both free ligands resulting from geometry optimizations are collected in Table 5. In parentheses are given the values of these distances obtained from the crystallographic structure determinations described above. The $M-N_{pyrazine}$ distance is compared with the average $M-N_{pyrazine}$ distance in the tpza complex.

The overall computed geometries of all acetonitrile-containing species are similar, belonging to the C_3 symmetry group, with the 3-fold axis passing through the M−NCC direction. The ADF program does not handle this symmetry group, and consequently, all computations on these species were carried out without symmetry simplifications. The computed geometries of the pyrazine derivatives do not exhibit any symmetry, owing to the dihedral angle between the MI_3 fragment and the pyrazine ring.

As shown in Table 5, several differences appear in the structural parameters of Ln and U species. For a given lanthanide, the M−N distances are very similar for acetonitrile (La−N = 2.59 Å, Nd−N = 2.52 Å) or pyrazine (La−N = 2.63 Å, Nd−N = 2.52 Å). The decrease in the value of the M−N distances (0.07 Å for MeCN and 0.08 Å for pyrazine) from La to Nd is in agreement with the expected contraction (0.066 Å) calculated from Shannon ionic radii.[62] These observations are consistent with a mainly ionic interaction between the lanthanide cation and the ligand.

Altough the value of the ionic radius of U(III) is very similar to that of La(III), the uranium complexes exhibit shorter M−N distances for the acetonitrile (2.26 Å) and pyrazine (2.35 Å) species. These values are much shorter than the experimental data, but it must be emphasized that in these model compounds the coordination number is also much lower than in the crystallized complexes. Nevertheless, the significant result is not the values of the distances in themselves, but the observation of a decrease in the M−N distances from La to U, for both ligands, which reproduces the trend found in the crystal structures.

Moreover, this finding should be considered with the observation of a lengthening of the C−N bond in the uranium model species, 1.19 Å, as was observed in the crystallographic structure (1.19 Å), compared to the C−N distance calculated in both lanthanide homologues, 1.16 Å (crystallographic structure, 1.13 Å). No lengthening of the C−N bond could be detected in the pyrazine species, but the strain due to the aromatic ring precludes any significant modification in the bond lengths.

The trends in the M−N and C−N interatomic distances, either calculated or experimental, strongly suggest that some back-bonding may occur in the uranium complexes. We have therefore performed a detailed analysis of the orbital interactions to gain a better understanding of the bonding. At this point, it should be stressed that although KS orbitals are primarily mathematical intermediates to express the electron density, it has been shown that they give a reliable description of the MOs of a chemical system (for a recent discussion see ref 63 and references therein).

The description of the KS orbitals has been performed on a per-fragment basis, as implemented in ADF, to get a straightforward chemical analysis, starting from the metal cation M^{3+}, the iodide anions, and the nitrogen ligand. In Table 6 are reported the KS eigenvalues as well as the main fragment orbital contributions to the molecular orbitals, for the MI_3–acetonitrile species (M = La, Nd, U). In the case of unrestricted calculations, only the α part is shown.

For La and Nd, no significant orbital interaction between the MI_3 species and the acetonitrile ligand is observed. Some weak σ- and π-donation of the iodide ions to the 5d, 6p, and 4f orbitals of the Ln^{3+} fragment occurs, as can be seen from the detailed analysis of the group of MOs between ca. −7 and −6 eV, which are mainly based on 5p (I) orbitals. The expected decrease in the energy of the 4f orbitals is observed, from La (ca. −2.8 eV) to Nd (ca. −5.2 eV).

The uranium derivative has an electronic structure similar to those of the lanthanides, with a block of orbitals, mainly 5p (I), showing some donation to the uranium (6d, 7p, 7s, 5f) valence orbitals. The block of 5f-type orbitals lie above (between −4.25 and −3.9 eV) the 5p (I) orbitals, and the π^* CN virtual orbital is found at higher energy. Two of the three unpaired electrons in the uranium derivative occupy 5f-type orbitals, combined with 13% π^* CN from the

(62) Shannon, R. D. *Acta Crystallogr.* **1976**, *A32*, 751.

(63) Stowasser, R.; Hoffman, R. *J. Am. Chem. Soc.* **1999**, *121*, 3414.

Table 6. KS Orbital Energy Levels (eV) and Main Orbital Contributions (%) for I_3M−Acetonitrile Species (M = La, Nd, U)[a]

				other orbital contributions	
	E (eV)	occupation	main orbital type	M	L
LaI_3–L	−7.19 to −6.10	9 × 2	I (5p): 85−98%	10% 5s, 5−14% 5d, 5−3% 6p	
	−3.18; −3,19	0	L (π* CN): 100%		
	−2.78 to −2. 59	0	La (4f)		
NdI_3–L	−6.93 to −6.23	9 × 2	I (5p): 88−98%	11% 6s, 4−8% 5d, 2−5% 6p, 10% 4f	
	−5.28; −5.25; −5.23	3 × 1 (α electrons)	Nd (4f): 100%		
	−5.19 to −5.07	4 × 0	Nd (4f): 100%		
	−3.01; −2.99	2 × 0	L (π* CN): 100%		
UI_3–L	−10.0 to −6.45	9 × 2	I(5p): 85−100%	13% 7s, 8−14% 5d, 3−5% 7p, 5% 5f	
	−4.25	1 × 1 (α electron)	U (5f): 90%	9% 7s	
	−4.11; −4.108	2 × 1 (α electrons)	U (5f): 85%		13% π* CN
	−3.99 to −3.93	4 × 0	U (5f): 100%		
	−3.096; −3.086	2 × 0	L (π* CN): 80%	12% 5f	

[a] The occupation gives the number of molecular orbital levels times the number of electrons in these orbitals.

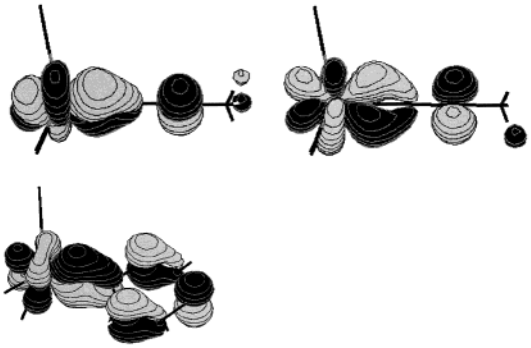

Figure 3. (a, top) Two highest occupied molecular orbitals of UI_3–acetonitrile, showing the 5f−π* CN interaction. (b, bottom) Molecular orbital of UI_3–pyrazine showing the 5f−π* CN interaction.

acetonitrile fragment, while the third electron is found in a pure 5f orbital. This orbital interaction is represented in Figure 3a, where both highest KS orbitals are shown, each with one component of the π* CN orbital overlapping with the symmetry-related 5f orbital. This result points to a π-back-donation from the 5f electrons to the π* CN virtual orbital of the acetonitrile.

It is worth noting that the presence of this orbital interaction is not merely an effect of the M−N distance. To show this, we have performed a computation of the electronic structure of the NdI_3–acetonitrile derivative using the same distance (i.e., Nd−N = 2.26 Å) as in the uranium analogue. The electronic structure obtained is the same as the one in the equilibrium geometry, and no 4f−acetonitrile interaction could be observed. Along the same line, we have also studied the UI_3–acetonitrile species using a longer U−N distance, corresponding to that in the neodymium derivative (2.52 Å). The resulting electronic structure is very similar to the one described above for the fully optimized structure, the only difference being a weaker amount of mixing of the π* CN orbital with the 5f orbital, ca. 8%, which is consistent with the longer $U-N_{acetonitrile}$ bond.

Similar behavior is observed for the pyrazine complexes: the general trends are essentially the same as for the acetonitrile derivatives. No orbital interaction between the lanthanide cation and the pyrazine ligand was observed, whereas in the uranium derivative, a nonnegligible mixing, i.e., 33%, occurs between one of the occupied symmetry-adapted 5f orbitals and the π* MO of the pyrazine ring: see Figure 3b for a representation of this interaction. The electron transfer amounts to 0.33 e as given by the Mulliken population analysis, and it is thus higher than with the acetonitrile ligand.

Table 7. Mulliken and Hirschfeld Charges for M^{3+}, I^-, and L Initial Fragments[a]

	Mulliken			Hirschfeld		
	M^{3+}	L	I^-	M^{3+}	L	I^-
L = Acetonitrile						
LaI_3–L	1.12	0.12	−0.42	2.34	0.03	−0.79
NdI_3–L	1.14	0.10	−0.41	2.28	0.03	−0.77
UI_3–L	1.17	−0.27	−0.30	2.53	−0.22	−0.77
L = Pyrazine						
LaI_3–L	1.14	0.15	−0.43	2.34	0.06	−0.80
NdI_3–L	1.12	0.14	−0.42	2.29	0.05	−0.78
UI_3–L	1.08	−0.24	−0.28	2.56	−0.25	−0.77

[a] L = acetonitrile, pyrazine; M = La, Nd, U.

The examination of atomic and molecular charges corroborates the difference evidenced here between the Ln(III) and U(III) complexes. The Mulliken gross charges are summarized in Table 7 together with the charges derived from the Hirschfeld analysis, i.e., the integral for each fragment of ρ(SCF)ρ(frag)/ρ(sum of fragments). The charge of the metal cation is similar for both lanthanides, meanwhile the charge on the ligand, very slightly positive for the lanthanide complexes (ca. +0.01 to +0.04 e), becomes negative (ca. −0.25 e) for the uranium complexes. These trends are similar for both charge analyses. In view of this difference in interaction between lanthanides and uranium, it becomes interesting to compare the amount of energetic stabilization gained when the ligand is bonded to LnI_3 and to UI_3 species. We have used the per-fragment energetic analysis of ADF, starting from M^{3+}, I^-, and L fragments, for the calculation of the energy terms (see the Computational Details).

One drawback of this procedure is that all starting fragments must be closed-shell. In our case, it was thus necessary to carry out two calculations: the first one was carried out for MI_3–L, starting from M^{3+}, I^-, and L fragments, and the second one for MI_3 starting from M^{3+} and I^-, with the optimized geometry obtained for MI_3–L.

The values obtained for all complexes are shown in Table 8. The basis set superposition errors (BSSEs), estimated by the counterpoise method, are all smaller than 0.8 kcal/mol

Table 8. Energy Analysis (kcal/mol) of the MI_3–L Interaction: Total Bonding Energy (E_{TBE}) and Steric (Pauli + Electrostatic) and Orbital Components[a]

	E_{TBE}	E_{Pauli}	E_{elec}	E_{ster}	E_{orb}
L = Acetonitrile					
LaI_3–L	−24.6	32.1	−54.9	−22.8	−1.8
NdI_3−L	−24.8	33.0	−55.7	−22.7	−2.0
UI_3–L	−37.5	102.2	−88.5	13.7	−51.2
L = Pyrazine					
LaI_3–L	−25.8	32.8	−52.3	−19.5	−11.3
NdI_3–L	−26.4	44.4	−58.6	−14.2	−12.3
UI_3–L	−39.0	114.3	−95.6	18.7	−57.8

[a] Both fragments, MI_3 and L, are taken at the molecular optimized geometry.

Chart 2

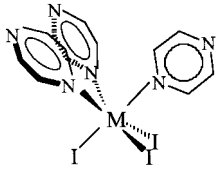

in absolute value, and zero-point energy (ZPE) corrections are close to −1 kcal/mol for all complexes.

Both uranium species have a higher total bonding energy (ca. −38 kcal/mol) than the lanthanide homologues, which all give similar values (ca. −25 kcal/mol). For lanthanide complexes, the steric term is negative whereas the orbital term is almost zero. The equilibrium lanthanide−N distance is merely the result of the balance between the repulsive Pauli interaction and the attractive electrostatic interaction. The conclusion which can be drawn is that the stabilization of LnI_3–L species is essentially electrostatic. In contrast, in uranium derivatives the steric contribution is positive, because of the short U−N distance. Nevertheless, despite this positive steric energy, the uranium complexes are stabilized, and this energy gain comes from the orbital term, which is highly negative, compared to that of the Ln species. We can therefore conclude that the electron transfer observed in the case of the trivalent uranium species with N-donor ligands results in an overall stabilization effect compared to the lanthanide homologues.

These simple model compounds allow a precise determination of the structural and electronic features of the metal−ligand interaction. Moreover, they are appropriate for applying more accurate methodologies such as CAS or four-component calculations, which we are currently investigating. However, the low coordination number of the metal (CN = 4) in these simple model systems overemphasizes the difference between U−N and L−N distances. To get a better agreement with the experimental data, we have studied the more complete model system [I_3M(pyrazine)$_3$] (Chart 2) in which the metal center has a higher coordination number (CN = 6).

To simplify the calculations, a C_{3v} symmetry was imposed to the structure and a partial optimization of the M−N bond length was carried out, keeping the other interatomic distances constant at the averaged experimental values, i.e., M−I = 3.2 Å, with the angle between the C_3 axis and the M−N bond equal to 63° and the angle between the C_3 axis and the M−I bonds equal to 115°. The metal−$N_{pyrazine}$ equilibrium distances thus obtained are 2.60 Å for U and 2.72 Å for the La analogue, with a decrease of the M−N bond length from La to U of 0.12 Å. This value is closer to the experimental one than the one found in the simpler models. This corroborates our assumption that the strong contraction in the metal−$N_{pyrazine}$ (ca. 0.28 Å) distance, from La to U, that was obtained with the small model I_3M−L is mostly due to the low CN. Note that the CN in the I_3M(pyrazine)$_3$ model (CN = 6) is still lower than in the crystallographic structures (CN = 8). This difference in coordination number and the additional sterical contraints imposed by the tripodal structure in the experimental system are probably the cause of the remaining differences between the calculated and experimental distances. We also performed on this more complex model an electron structure analysis in terms of fragment charges and composition of main KS orbitals. An energetic decomposition of the total bonding energies based on MI_3 and three pyrazine starting fragments was also carried out. In Table 9 are reported the charge analyses and the energetic decomposition, for M = La and U.

Table 9. Electron Structure Analysis (SFOs and Atomic or Molecular Charges) and Energetic Decomposition (kcal/mol) for MI_3(pyrazine)$_3$ Species

	M = La	M = U
Mulliken Charges		
M	1.31	1.42
pyrazine	0.09	−0.02
I	−0.53	−0.45
Hirschfeld Charges		
M	2.38	2.53
pyrazine	0.04	−0.04
I	−0.83	−0.80
Bonding Energy		
E_{TBE}	−57.3	−63.7
E_{orb}	−26.8	−61.1
E_{elect}	−141.9	−180.4
E_{ster}	−30.5	−2.6

A close examination of our results leads to the same conclusions drawn for the small model compounds. It shows a back-donation from the uranium 5f orbitals to the virtual π^* orbital of the pyrazine rings, with a 0.12 e transfer to each ligand, as given by the Mulliken population analysis. The energetic analysis also reflects the stabilization due to this orbital interaction in the case of the uranium ion.

Discussion

The crystal structures of two trisiodide octacoordinated uranium(III) complexes of tpza which differ only by the ligand occupying the eighth coordination site (thf or MeCN) and of their lanthanum(III) analogues have been determined. In the acetonitrile adducts the M−$N_{pyrazine}$ and M−I distances are very similar for U(III) and La(III), with the largest ΔLa−U values equal to 0.019 for $N_{pyrazine}$ and 0.017 for I (Table 3). These values confirm that the radii of U(III) and La(III) are very similar in molecules with the same coordination number. The U−$N_{acetonitrile}$ distance is 0.05 Å shorter than the La−$N_{acetonitrile}$ one. A lengthening of the N≡C bond

in the coordinated acetonitrile molecule is also observed in the U complex with respect to the La one. This suggests the presence of a U(III)−acetonitrile π-back-bonding interaction. The presence of a back-donation from the metal to acetonitrile has been described before for transition-metal nitrile complexes. A decrease of the η^1-coordinated nitrile stretching frequency with respect to the free ligand value had been reported for pentaammineruthenium(II)−nitrile complexes[64] and attributed to unusually strong metal−acetonitrile π-back-bonding interactions. The crystal structure of the pentaammineruthenium(II)−benzonitrile complex shows a small lengthening of the N≡C bond in the coordinated benzonitrile (1.16(8) Å) with respect to that of the pentaammineruthenium(III)−benzonitrile complex (1.130(6) Å). A larger lengthening of the N≡C bond is observed in Mo and W complexes containing bent organonitriles coordinated in a side-on fashion, and computational studies have shown the presence of a strong back-bonding interaction between the η^2-coordinated nitrile and the metal.[65]

In the [M(tpza)I_3(thf)] complexes in which the monodentate ligand acetonitrile, a weak π-acceptor ligand, is replaced by a thf molecule, a σ-donor only, the mean value of the distance U−$N_{pyrazine}$ is 0.05 Å shorter than the mean value of the La−$N_{pyrazine}$ distance. Since we are comparing isostructural compounds of ions with very similar ionic radii, these differences indicate the presence of a stronger M−N interaction in the U(III) complexes and therefore suggest the presence of a covalent contribution to the U−N bonding. The differences observed are rather small but significant since they are larger than the difference found for M−O (0.025 Å) and M−I (0.033 Å) (Table 4) and they are also larger than the largest ΔLa−U difference observed for $N_{pyrazine}$ (0.019 Å) in the [M(tpza)I_3(MeCN)] complexes. Moreover, these small differences are consistent with the weak π-acceptor character of pyrazine. Structural evidence of the ability of U(III) to act as a π-donor with strong π-accepting ligands such as phosphine, phosphite, or isocyanide has been previously reported by Brennan and co-workers.[8] For these ligands differences of ∼0.1 Å were observed between U(III)−L (L = PMe_3 or CNEt) and Ln(III)−L distances. The structural differences that we expect with aromatic heterocyclic N-donors are therefore smaller in view of their weaker π-accepting abilities. Moreover, the results presented here show that the interaction U−N_{tpza} is modulated by the other ligands present in the coordination sphere of the metal, which is consistent with the presence of a covalent contribution to the U−N bond. In the presence of weakly π-acid ligands such as acetonitrile or pyridine, we do not observe significant differences in the M−tpza interaction between U(III) and La(III), with similar M−N_{tpza} bond distances being found for the acetonitrile-containing M(tpza)I_3 complexes **1** and **2** and with similar formation constants being measured for U(tpza)I_3 and La(tpza)I_3 in pyridine. On the other hand, in the presence of the ligand thf, which can only act as a σ-donor and then cannot compete with tpza for the electron density of the metal, a stronger M−N_{tpza} interaction is observed for U(III) with respect to La(III) in solution and in the solid state.

The DFT calculations presented here do support the presence of a covalent U(III)−N-donor ligand bonding due to some back-donation from U 5f orbitals to π^* C−N orbitals. They are able to reproduce the experimental structural trends concerning the shortening of the metal−N distances from Ln to U combined with the lengthening of the CN bond in the uranium−acetonitrile compound. Such back-bonding interactions are probably due to the low valence state of uranium, which results in high-energy 5f valence orbitals, and are not expected to occur with higher oxidation states (≥IV). Heavier actinides, where the 5f orbitals lie lower in energy, may not exhibit this kind of interaction.

To summarize, the computational results highlight the balance between two competing effects in the metal−ligand equilibrium distance: the steric repulsion and the electrostatic/covalent attractive interaction. This phenomenon is quantified by the energy decomposition analysis. The additional back-donation interaction in the case of uranium leads to an increase of the total bonding energy compared to the lanthanide homologues. This occurs despite an increased Pauli repulsive part due to the very short U−N distance.

Conclusion

Two principal results have been described and discussed here. A significant shortening of the M−$N_{acetonitrile}$ and M−$N_{pyrazine}$ distances has been found for U(III) with respect to La(III) in the complexes described, while the ionic radii of La(III) and U(III) are similar. This is the first report of significant structural differences in analogous U(III) and Ln(III) complexes containing neutral N-donor ligands, and suggests the presence of a covalent contribution to the U−N bond.

The structural differences observed in the crystal structures of the tpza complexes presented here are larger than the differences observed in the complexes of tpa previously described, indicating the presence of a stronger U(III)−$N_{heterocyclic}$ π-back-bonding interaction for tpza. Moreover, we have shown that the U(III)−$N_{heterocyclic}$ interaction is stronger in the presence of σ-donor-only ligands than in the presence of weak π-acceptors. Structural studies on U(III) and Ln(III) complexes of aromatic heterocyclic N donors with similar or increased π-acid character in the presence of ligands acting only as strong donors will allow the presence of a covalent contribution to the U−$N_{heterocyclic}$ bonding to be further substantiated.

The second point is the ability of the theoretical density functional study to reproduce experimental trends on one hand, and to give a description of the bonding in either Ln(III) or U(III), consistent with all experimental data, on the other hand. Further theoretical studies are now under way on the more complete models to check the ability of other approximate relativistic methods to reproduce experimental

(64) Clarke, R. E.; Ford, P. C. *Inorg. Chem.* **1970**, *9*, 227.
(65) Wadephol, H.; Arnold, U.; Pritzkow, H.; Calhorda, M. J.; Veiros, L. *J. Organomet. Chem.* **1999**, *587*, 233.

trends and the nature of the metal−ligand interaction in f element complexes.

Acknowledgment. This work was supported by the Commissariat à l'Energie Atomique, Direction de l'Energie Nucléaire. We thank Lydia Karmazin for the determination of the $K_{U(tpza)}/K_{La(tpza)}$ ratio and Carlo Adamo (ENSCP, Paris) for fruitful discussions.

Supporting Information Available: Complete tables of crystal data and structure refinement, atomic coordinates, bond lengths and angles, anisotropic displacement parameters, and hydrogen coordinates for compounds **1**−**4**. This material is available free of charge via the Internet at http://pubs.acs.org.

IC010839V